

Dissociative Low-Energy Electron Attachment to the C–S Bond of H₃CSCCH₃ Influenced by Coulomb Stabilization

Monika Sobczyk,^{1,2} Piotr Skurski^{1,2} and Jack Simons¹

¹Chemistry Department, Henry Eyring Center for Theoretical Chemistry, University of Utah, Salt Lake City, UT 84112, USA

²Department of Chemistry, University of Gdansk, 80-952 Gdansk, Poland

Abstract

In earlier works by our group, it was suggested that the presence of stabilizing Coulomb potentials can allow low-energy electrons (i.e., with kinetic energies < 1 eV) to attach to σ^* orbitals of certain bonds and to thus cleave those bonds. In these earlier efforts, we focused on SS bond cleavage and in breaking a variety of bonds that occur in typical peptides and proteins. In the present effort, we focus primarily on the stabilizing effects of nearby positive charges on the electron attachment process to dimethyl sulfide (DMS) to break one of the C–S bonds. *Ab initio* electronic structure calculations have been used to explore the influence of Coulomb potentials on the ability of low-energy electrons to directly attach to the σ^* orbital of the C–S bond and to effect bond cleavage, as well as to examine σ^* anion energy evolution as a function of C–S bond length.

Contents

1. Introduction	239
2. Methods	242
3. Results	245
4. Summary	249
Acknowledgements	250
References	251

1. INTRODUCTION

There exist a variety of experimental mass spectrometric methods for effecting fragmentation of gas-phase charged samples of a wide range of organic and inorganic systems. Because of their ability to cause very specific and limited bond cleavages, electron capture dissociation (ECD) [1–4] experiments, where very low-energy electrons are attached to the gaseous sample after which specific bonds break, have shown great promise.

Recent studies carried out by our group show [5] that low-energy electrons can directly attach to and subsequently fragment S–S σ bonds in disulfide-linked dimers of Ac-Cys-Ala_{*n*}-Lys (with *n* = 10, 15, and 20) that are protonated at their two Lys sites. An example of such a species is shown in Fig. 1 where the alanine

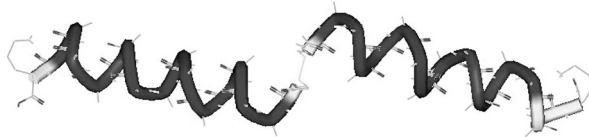


Fig. 1. Structure of an $(\text{AcCA}_{15}\text{K}+\text{H})_2^+$ disulfide-linked dimer [6]. The disulfide linkage is at the center and the two protonated sites are at the left and right ends.

helices are marked red, the cystine linkage containing the S–S bond appears in the center, and the two Lys sites are at the termini.

According to the mechanism treated in Ref. [5], an excess electron enters the S–S antibonding σ^* orbital to form a metastable anion that can either undergo electron auto-detachment at a rate $> 10^{14} \text{ s}^{-1}$ or fragment (promptly because of the repulsive nature of the σ^* anion's energy surface) to form an R–S radical and an $^- \text{S–R}'$ anion. The yield of bond cleavage per attached electron is governed by competition between fragmentation on the σ^* surface and the auto-detachment process. The *ab initio* calculations of Ref. [5] were carried out on a very simple model of the disulfide shown in Fig. 1, the $\text{H}_3\text{C–S–S–CH}_3$ molecule. The R–S–S–R' neutral and corresponding anion potential energy curves for dimethyl disulfide as functions of the S–S distance are depicted in Fig. 2.

The data shown in Fig. 2 suggest that the near vertical attachment of an electron into the S–S σ^* orbital of MeS–SMe would require an electron with kinetic energy of *ca.* 0.9 eV and would generate the σ^* anion on a reasonably repulsive part of its energy surface. This results in the well-known dissociative electron attachment (DEA) process [7,8] which has been well studied experimentally for MeS–SMe. Figure 2 also suggests that lower-energy electrons can attach to the σ^* S–S orbital

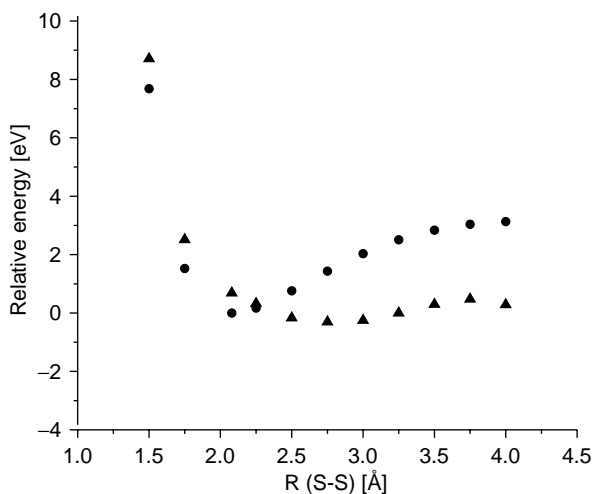


Fig. 2. Energies of the dimethyl disulfide neutral (circles) and σ^* anion (triangles) as functions of the S–S bond length (Å) with all other geometrical degrees of freedom relaxed to minimize the energy.

but only if the S–S bond is stretched to near 2.25 \AA , which would require *ca.* 0.5 eV of vibrational excitation. Of course, except at considerably elevated temperatures, such high vibrational excitation is extremely improbable. So, the most likely means by which electrons can enter the S–S σ^* orbital of a room-temperature sample is to have *ca.* 0.9 eV of kinetic energy and to do so in a near vertical manner.

The effects that proximal positively charged groups can have on the DEA process were the primary focus in Ref. [5]. Specifically, we considered the Coulomb stabilization that one or more nearby positive groups (e.g., simulating the protonated Lys sites in the molecule shown in Fig. 1) can have on the nascent σ^* anion. As an example of the effects of Coulomb interactions, in Fig. 3 we show the MeS–SMe neutral and MeS–SMe $^-$ σ^* anion potentials as in Fig. 2 but calculated in the presence of two $+1$ charges each 30 or 10 \AA from the midpoint

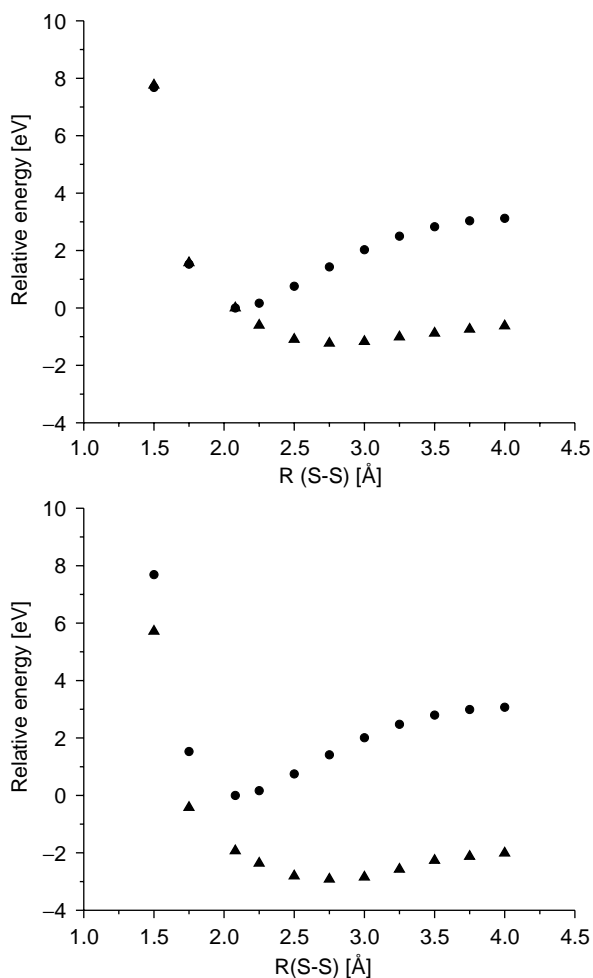


Fig. 3. Neutral (circles) and σ^* anion (triangles) curves of MeS–SMe in the presence of two $+1$ charges 30 \AA (top) and 10 \AA (bottom) from the midpoint of the S–S bond.

of the S–S bond (i.e., one +1 charge on one side of the bond and the other +1 charge in the opposite direction). Clearly, in comparison with Fig. 2, the σ^* anion curves in Fig. 3 are lowered in energy by a substantial amount relative to the energy of the neutral. This causes the anion curve to intersect the neutral at smaller S–S separations (e.g., at bond lengths that may be accessed in the zero-point vibration of the S–S bond) and at much lower energy.

We have observed that the energy lowering of the σ^* anion curve can, in fact, be estimated in terms of the Coulomb potential produced by the two +1 charges. For example, when the two charges are 30 Å distant, the Coulomb energy at the midpoint of the S–S bond is $2(14.4 \text{ eV } \text{Å}/30\text{Å})=0.96 \text{ eV}$; when the two charges are 10 Å away, the Coulomb stabilization energy is 2.88 eV. The rigidity of the compounds shown in Fig. 1 caused by their helical subunits allowed us to accurately know the distances between the S–S bond and the two +1 sites, so these species provided excellent support for postulate that our model MeS–SMe compounds were designed to probe.

Based upon the results of such studies, we suggested in Ref. [5] that Coulomb potentials produced by nearby positive charges could stabilize the σ^* metastable anion states to an extent that might render them electronically stable. Under such circumstances, the endothermic DEA process illustrated in Fig. 2 might be made exothermic or thermo-neutral and thus able to effect bond breakage at a much higher yield. The data of Fig. 3 suggest that S–S σ bonds, which require electrons of *ca.* 0.9 eV to induce DEA in the absence of positive charges, can attach essentially zero-energy electrons to produce S–S bond cleavage if two +1 charges are within 30 Å (or, equivalently, if one +1 charge were within 15 Å).

Our suggestion that proximal positively charged groups can substantially alter the energy requirements and efficiencies of DEA processes can be of great significance to workers who study electron-induced bond fragmentation propensities in, for example, gas-phase mass spectrometric (including ion-cyclotron resonance) experiments on charge peptides and proteins. In particular, the use of ECD [1–4] methods for fragmenting such bio-molecules gives rise to very specific bond-cleavage patterns but the mechanisms involved are not yet fully understood. In fact, an unusual outcome [6] in ECD experiments on the kind of molecule shown in Fig. 1 is what motivated us to examine the effects of Coulomb stabilization in the first place.

To extend our previous studies of such processes, we decided to examine in the present effort the anion that results from attaching an electron to the C–S σ^* orbital of Me–S–Me shown in Fig. 4 as well as the neutral and anion energy surfaces associated with cleaving the C–S bond in the absence and presence of two positive +1 charges at 10, 20, and 30 Å.

2. METHODS

Prior to stretching C–S bond, we optimized the geometry of the anionic Me–S–Me[−] molecule and parent neutral molecule at the unrestricted second-order Møller–Plesset (UMP2) perturbation level of theory (in order to take into account the effect of electron correlation) with aug-cc-pVDZ basis sets [9]. We also

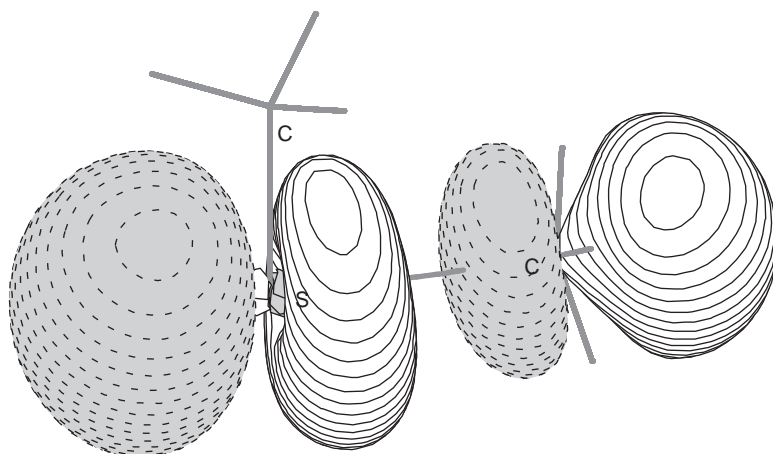


Fig. 4. The singly occupied σ^* molecular orbital of the C–S bond (at $R_{\text{CS}} = 2.5 \text{ \AA}$) that holds the excess electron of the Me-S-Me^- anion.

calculated all vibrational frequencies of the neutral and anionic species to make sure the structures thus found were indeed minima on the energy surface.

In addition, to generate the neutral molecule and anion energies as functions of the C–S bond length (R), we performed such UMP2 calculations at a range of R -values using partial geometry optimization, with only the C–S bond distance frozen and all other geometrical degrees of freedom relaxed to minimize the energy. In all calculations, the values of $\langle S^2 \rangle$ never exceeded 0.7780 (after annihilation) for the doublet states, so we are confident that spin-contamination effects do not have significant influence on our results.

The anion calculations are especially problematic at R -values, where the anion's energy lies above that of the neutral (i.e., when the anion is metastable). In such cases, great care must be taken to avoid having the anion's wave function undergoing variational collapse (i.e., to describe an electron distant from the neutral molecule and having little kinetic energy). When stretching the C–S bond, we had to be careful to monitor the anion's orbital occupancy to guarantee that the σ^* orbital was indeed the singly occupied molecular orbital. At large R -values, this is rather straightforward because, at such distances, the anion is electronically stable. However, at R -values where the C–S σ^* anion's energy lies above that of the neutral molecule, we had to employ special techniques for such an electronically metastable state.

In the method we used to overcome these problems for metastable anions, we increased the nuclear charges on the two atoms (e.g., C and S, when stretching the C–S bond) involved in the bond cleavage by an amount δq and carried out the anion and neutral calculations. These increased nuclear charges cause the C–S σ^* anion state to be differentially lowered in energy and to thus become electronically stable relative to the neutral molecule. In this way, we were able to make sure that the anion energy and orbital occupancy we obtained in our UMP2 calculations corresponded to the proper σ^* anion. By employing this δq

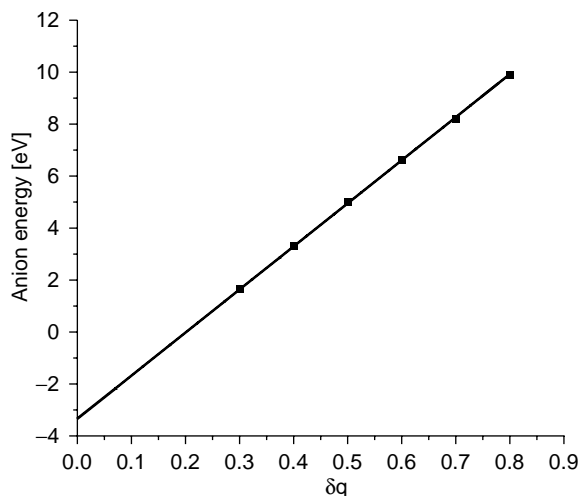


Fig. 5. Plot of the energy of the anion relative to that of the neutral in which an electron is in a C–S σ^* orbital vs. the stabilizing partial charge δq added to the C and S atoms.

charge-increase technique for a range of δq values (e.g., $\delta q = 0.1$ – 1.0 was typical) within which the σ^* anion is electronically stable, we could then plot the stable energies $E(\delta q)$ of the σ^* anion vs. δq and extrapolate to $\delta q = 0$ to evaluate the metastable σ^* anion's energy. An example of such an extrapolation is shown in Fig. 5.

As a result of such a treatment, we were able to compute the electronic energy of the neutral Me–S–Me molecule as a function of the C–S bond length as well as the electronic energy of the anion state of interest at all R -values. In particular, we were able to evaluate the anion's energy both at geometries where it is electronically stable and where it is metastable, the latter being especially important for estimating the vertical electron attachment energies that relate to DEA processes.

In addition to carrying out such calculations in the absence of any stabilizing Coulomb potentials, we repeated each calculation with Coulomb potentials present. In all such calculations, we placed two $+1$ charges at 10, 20, or 30 Å from the midpoint of the C–S bond, and repeated the evaluation of the neutral and anion energies.

Because we find that the presence of a $+1$ charge stabilizes the anion curves in a highly predictable manner (i.e., by lowering the σ^* curve by $14.4 \text{ eV}/R$, where R is the distance in Å to each $+1$ charge), we can predict the energy and shape of the σ^* anion curve for arbitrary values of the local Coulomb potential. This, in turn, allows us to utilize our findings to predict the effects, for example, of protonated adjacent groups whose distance to a given bond may even fluctuate as the molecule undergoes thermal motions. So, even though we carry out calculations for only certain strengths of the Coulomb potential, we suggest that our data can be used to predict under what Coulomb potentials a given bond will or will not be susceptible to exothermic DEA.

283 In the absence of additional positive stabilizing charges, the electronic
284 instability of the Me–S–Me[−] anion does not occur for C–S bond lengths larger
285 than 2.37 Å, where the excess electron is localized on the Me–S fragment. It is
286 known [10] that Me–S possesses a positive electron affinity of *ca.* 1.87 eV which
287 is 1.79 eV larger than the electron affinity of the methyl radical. This difference
288 in the values of the electron affinities directly influences the localization of the
289 excess electron on the Me–S–Me[−] anion during fragmentation. When two
290 positive +1 charges are present, the anionic energy curve is shifted down to lower
291 energies where it remains ‘below’ the corresponding neutral energy curve for C–S
292 bond lengths larger than 1.95 Å. This is because the anion with the singly
293 occupied σ^* orbital shown in Fig. 4 is stabilized by the electrostatic Coulomb
294 potential of the positive point charges added.

295 All of our calculations were performed with the Gaussian98 suite [11] of codes
296 on AMD Athlon 2000+ 1.6 GHz and Pentium IV 1.7 GHz computers, as well as
297 on SGI Origin2000 and Compaq Sierra systems. The three-dimensional plots of
298 molecular orbitals were generated with the MOLDEN program [12].
299
300
301

302 3. RESULTS 303

304 Before discussing the significance of our data, we wish to point out that the C–S
305 bond is a reasonably strong σ bond. As a result, the σ^* anion curve lies high above
306 the neutral curve near the equilibrium bond length of the neutral parent molecule.
307 Therefore, the σ^* anion state has a high energy and a correspondingly very short
308 lifetime (*ca.* 10^{-14} s or shorter). The short lifetime produces a very broad
309 Heisenberg width and thus makes the determination of the center of the DEA
310 cross-section difficult to determine. Moreover, the short lifetime causes
311 detachment to overwhelm dissociation of the σ^* anion, thus making the bond-
312 cleavage yield of the DEA process very low. All of these issues conspire to make
313 DEA data on the bond we are studying very scarce but still existent.
314

315 In Fig. 6 we show how the electronic energies of the neutral and anionic
316 systems vary along the C–S bond length with all other internal geometry
317 parameters relaxed to minimize the neutral or anion energy, respectively. These
318 plots allow us to examine where the anion’s energy surface lies relative to that of
319 the neutral, which obviously, is directly germane to attachment of a free electron
320 to the σ^* orbital of the C–S bond.

321 Examining the data used to create Fig. 6 in comparison with known
322 experimental values, we conclude that:

- 323
324 (i) The dissociation energy for Me–S–Me \rightarrow MeS + Me is 3.28 eV. The
325 experimental estimate of this energy derived from the laser photodissociation
326 and photoionization of DMS is 3.25 ± 0.06 eV [13].
327 (ii) The electron affinity of MeS is estimated to be 1.81 eV. This value is also in
328 reasonable agreement with the experimental value [10] of 1.87 eV. So, we
329 believe that our calculations provide satisfactory results in this case.

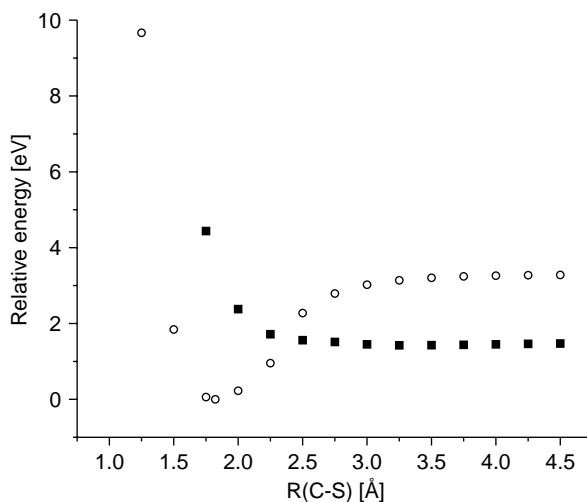


Fig. 6. Neutral (circles) and σ^* anion (squares) energies as functions of the C–S bond length in the absence of stabilizing charges.

We note that the σ^* anion lies 3.80 eV above the minimum of the neutral species in our calculations, which is somewhat higher than the experimentally determined 3.25 eV value in the DEA yield spectrum [7] (although this peak is 0.5 eV broad). We also note that the anion and neutral curves cross *ca.* 1.63 eV above the neutral's minimum. This amount of energy seems to be too high for vibrational excitation of the C–S bond to access at room temperature and thus accessing this crossing point remains unrealizable except at considerably elevated temperatures.

In Fig. 7 we show the corresponding neutral and anion curves (n.b., computed at the unrestricted MP2 level) associated with cleaving of the C–S bond when two +1 charges are located 10 Å from the midpoint of the bond being cleaved. The positive charges are used to represent the Coulomb potential presented by two protonated amine sites as, for example, in the dication in Fig. 1.

We see that in Fig. 7 the anion is electronically stable for values of C–S bond larger than 1.95 Å. The anion and neutral curves cross *ca.* 0.16 eV above the neutral's minimum. The amount of energy needed to access the crossing here is 10 times smaller than in Fig. 6 and thus can be thermally attainable at room temperature. Note that the energy of the anion relative to the neutral at $R=1.82$ Å (the neutral's R_e) moves from 3.80 eV in Fig. 6 to 1.08 eV in Fig. 7. This means that direct vertical attachment would require an electron to have *ca.* 1 eV of kinetic energy in this case. The 2.72 eV of Coulomb stabilization observed in this case is very close to that predicted by the equation for two positive charges at 10 Å: $2(14.4/(10+R_e/2))$ eV = 2.64 eV. This success of such simple Coulomb stabilization model may be surprising, but we remind the reader that this same kind of model has proven highly successful when used to predict electronic stabilities of anions in the past [14].

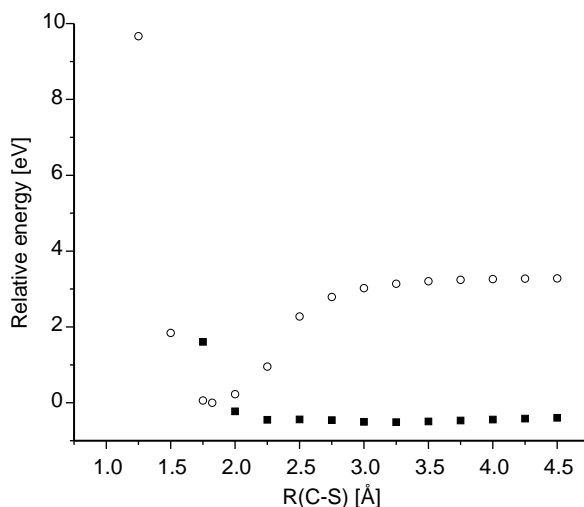


Fig. 7. Neutral (circles) and σ^* anion (squares) energies as functions of the C–S bond length when two positive +1 charges are located 10 Å from the midpoint of the bond.

Before examining the results obtained with the two +1 positive charges placed 20 or 30 Å from the midpoint of C–S bond, let us see what the Coulomb model predicts in those two cases. Specifically, it predicts the anion to be located relative to the minimum of the neutral at the following energies:

$$3.80 - 2(14.4/20.91) = 2.42 \text{ eV with the two } +1 \text{ charges } 20 \text{ \AA away}$$

$$3.80 - 2(14.4/30.91) = 2.87 \text{ eV with the two } +1 \text{ charges } 30 \text{ \AA away}$$

In Figs 8 and 9 we show the neutral and σ^* anion curves when two +1 charges are 20 or 30 Å from the C–S bond midpoint, and we note that these estimates are indeed quite good.

So, in the two latter cases we expect the C–S bond to be able to attach an excess electron, but only if the electron has 2.4–2.9 eV of kinetic energy or if the C–S bond is vibrationally excited by 0.7–1.0 eV.

Clearly, even when the two positive sites are only 10 Å away, the σ^* Me–S–Me anion is not electronically stable with respect to the neutral very near the equilibrium bond length of the neutral. Nevertheless, because the anion–neutral crossing occurs at low energy (i.e., 0.16 eV), direct electron attachment to the C–S bond to effect fragmentation seems to be possible when two positive sites are present and as distant as 10 Å and the C–S bond is elongated by vibrational motion. These findings and the Coulomb model that seems to be consistent with them suggest that when the two protonated sites are closer than *ca.* 6.67 Å, the σ_{CS}^* anion will be vertically stable [15] relative to the neutral, so direct electron attachment of zero-energy electrons would then not require any energy input (e.g., vibrational excitation to access the surface crossing).

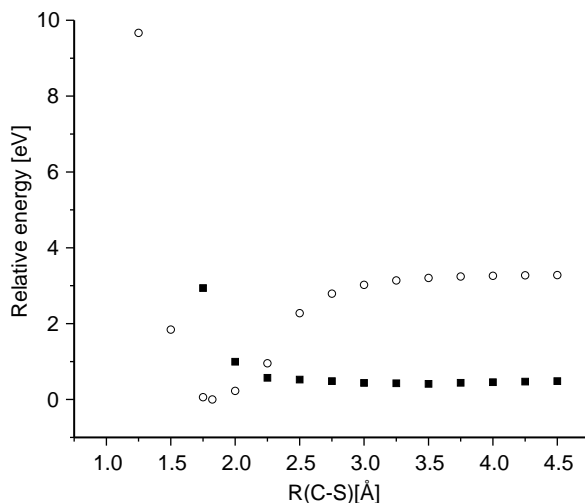


Fig. 8. Neutral (circles) and σ^* anion (squares) energies as functions of the C–S bond length when two +1 charges are located 20 Å from the midpoint of the bond.

Because the Coulomb potential plays a central role in the model outlined above, it seems important to examine the full electrostatic potential experienced by an electron as it approaches the C–S bond region. In Fig. 10 we show the electrostatic potential for Me–S–Me molecule in the absence of any positive charges, with blue denoting attractive regions and red labeling repulsive regions.

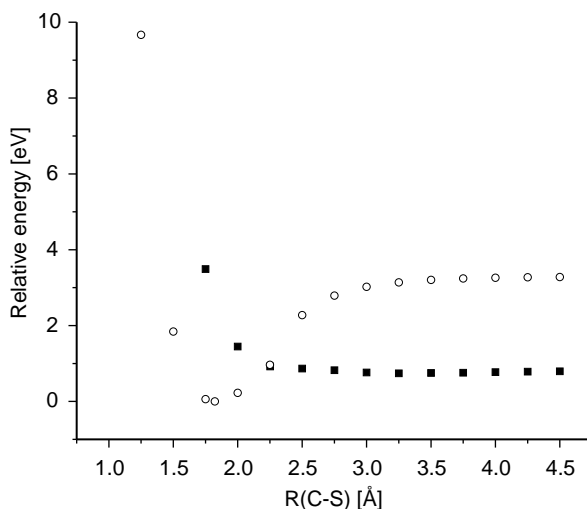
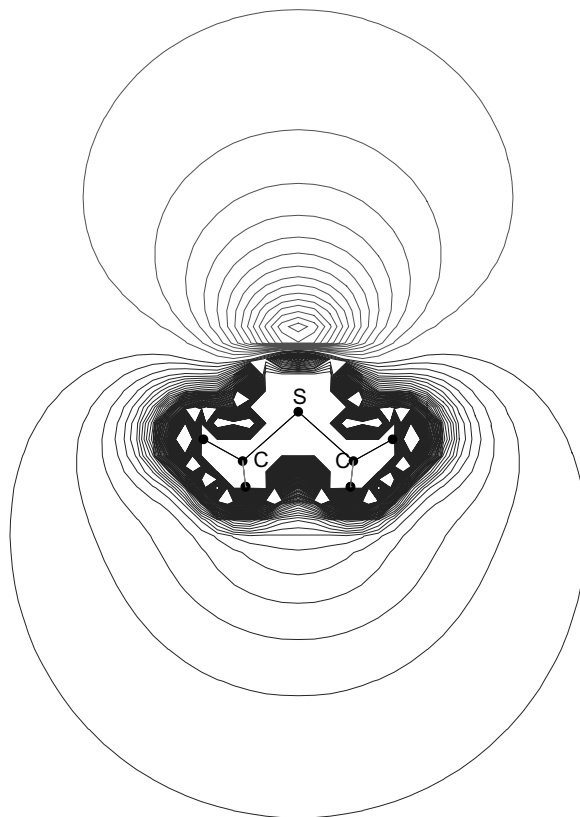


Fig. 9. Neutral (circles) and σ^* anion (squares) energies as functions of the C–S bond length when two +1 charges are located 30 Å from the midpoint of the bond.

471
472
473
474
475
476
477
478
479
480
481
482
483
484
485
486
487
488
489
490
491
492
493
494
495
496



497 **Fig. 10.** The electrostatic potential of Me–S–Me molecule. Red regions are repulsive to
498 an electron, blue are attractive.
499

500
501
502
503
504
505
506
507
508
509
510

The region where the lone pair orbitals of the sulfur atom reside is repulsive while the rest of DMS molecule is characterized by attractive potentials. There is no clearly attractive region near the C–S bond that would tend to guide an incident electron toward the σ_{CS}^* orbital because this figure corresponds to the equilibrium C–S bond length and the CS σ^* orbital lies high in energy. However, in cases where the two +1 positive charges are present at 10, 20, or 30 Å, an electron is most strongly attracted to regions near these positively charged sites where deep potential wells clearly exist, but our findings suggest that the region of the σ_{CS}^* orbital can also be attractive to such electron, especially when the C–S bond is elongated.

511
512
513

514 4. SUMMARY

515
516
517

Direct attachment of an electron to the σ^* orbital of the C–S bond of Me–S–Me shown in Fig. 4 has been examined using *ab initio* electronic structure methods.

518 Particular care has been devoted to establishing a qualitatively correct description
519 of the metastable anion state that arises.

520 For the situations in which a C–S bond is cleaved, so Me and MeS radicals are
521 formed, the corresponding Me–S[−] anion has a 1.81 eV positive electron binding
522 energy.

523 The vertical attachment of an electron to the σ^* orbital of this bond is highly
524 endothermic in the absence of Coulomb stabilization and requires the electron to
525 have a kinetic energy of *ca.* 3.80 eV (experiments probing the position of the σ^*
526 shape resonance give somewhat lower values). Even when Coulomb stabiliz-
527 ation of 2.88 eV is present (i.e., equivalent to two +1 charges 10 Å distant or
528 one +1 charge 5 Å away), the σ^* anion curve lies vertically 1.08 eV above the
529 neutral and intersects the neutral at a distance of 1.95 Å and 0.16 eV above the
530 neutral's minimum. It therefore seems unlikely that such strong σ bond will be
531 susceptible to cleavage by a direct low-energy (<3 eV) DEA mechanism when
532 positive charges are absent. To effect exothermic vertical attachment to such a σ
533 bond lying >3.80 eV above the neutral, one would have to have, for example, a
534 protonated amine site within 6.67 Å. Of course, one can imagine multiply
535 protonated species for which the total Coulomb stabilization at the σ bond site
536 could move that site's σ^* anion below the corresponding neutral, but such cases
537 are probably not common. The species shown in Fig. 1 represents such an
538 unusual case in which two +1 charges as distant as 30 Å are able to allow direct
539 DEA to occur. It is the weakness of the S–S bond (which causes the energy of
540 the σ^* orbital to be low lying) and the magnitude (*ca.* 1.8 eV) of the EA of the
541 S–R' radical formed upon bond cleavage that make this case special.

542 For the very strong C–S σ bond whose data are summarized in Figs 6–9,
543 the bond strengths and radical EAs do not combine to permit efficient direct
544 DEA when low-energy (i.e., <3 eV) electrons are involved. We therefore
545 expect that Coulomb-assisted C–S bond DEA will not be effective in gaseous
546 peptide samples except for bonds that happen to be very near two or more
547 protonation sites. That is, our data suggest that direct low-energy electron
548 attachment to and subsequent cleavage of the C–S σ bond is not likely except
549 for highly positively charged samples. So, the results presented here seem to
550 offer good insight into one aspect of the ECD process and they provide a
551 means by which one can estimate (based on a simple Coulomb energy
552 formula) which bonds may be susceptible to cleavage by low-energy electron
553 attachment.
554

555

556

557

558 ACKNOWLEDGEMENTS

559

560 This work was supported by NSF, Grant Nos. 9982420 and 0240387 to J.S., and
561 by the Polish State Committee for Scientific Research (KBN), Grant No. DS/
562 8371-4-0137-4 to P.S. Significant computer time provided by the Center for High
563 Performance Computing at the University of Utah and by the Academic Computer
564 Center in Gdansk (TASK) is also gratefully acknowledged.

REFERENCES

- 565
566
567 [1] R. A. Zubarev, N. Kruger, E. K. Fridriksson, M. A. Lewis, D. M. Horn, B. K. Carpenter and
568 F. W. McLafferty, *J. Am. Chem. Soc.*, 1999, **121**, 2857.
569 [2] R. A. Zubarev, D. M. Horn, E. K. Fridriksson, N. L. Kelleher, N. A. Kruger, M. A. Lewis,
570 B. K. Carpenter and F. W. McLafferty, *Anal. Chem.*, 2000, **72**, 563.
571 [3] E. A. Syrstad and F. Turecek, *J. Phys. Chem. A*, 2001, **105**, 11144.
572 [4] F. Turecek and E. A. Syrstad, *J. Am. Chem. Soc.*, 2003, **125**, 3353.
573 [5] A. Sawicka, P. Skurski, R. R. Hudgins and J. Simons, *J. Phys. Chem. B*, 2003, **107**, 13505.
574 [6] R. R. Hudgins, K. Håkansson, J. P. Quinn, C. L. Hendrickson and A. G. Marshall (unpublished
575 but in preparation). Although yet unpublished, these results have been presented in public at:
576 R. R. Hudgins, K. Håkansson, J. P. Quinn, C. L. Hendrickson and A. G. Marshall, *Proceedings*
577 *of the 50th ASMS Conference on Mass Spectrometry and Allied Topics*, Orlando, FL, June 2–6,
578 2002.
579 [7] C. Dezarnaud-Dandine, F. Bournel, M. Tronc, D. Jones and A. Modelli, *J. Phys. B: At. Mol.*
580 *Opt. Phys.*, 1998, **31**, L497.
581 [8] A. Modelli, D. Jones, G. Distefano and M. Tronc, *Chem. Phys. Lett.*, 1991, **181**, 361.
582 [9] R. A. Kendall, T. H. Dunning Jr. and R. J. Harrison, *J. Chem. Phys.*, 1992, **96**, 6796.
583 [10] J. C. Riensta-Kiracofe, G. S. Tschumper, H. F. Schaefer III., S. Nandi and G. B. Ellison, *Chem.*
584 *Rev.*, 2002, **102**, 231.
585 [11] M. J. Frisch, G. W. Trucks, H. B. Schlegel, G. E. Scuseria, M. A. Robb, J. R. Cheeseman,
586 J. A. Montgomery, Jr., T. Vreven, K. N. Kudin, J. C. Burant, J. M. Millam, S. S. Iyengar,
587 J. Tomasi, V. Barone, B. Mennucci, M. Cossi, G. Scalmani, N. Rega, G. A. Petersson,
588 H. Nakatsuji, M. Hada, M. Ehara, K. Toyota, R. Fukuda, J. Hasegawa, M. Ishida, T. Nakajima,
589 Y. Honda, O. Kitao, H. Nakai, M. Klene, X. Li, J. E. Knox, H. P. Hratchian, J. B. Cross,
590 C. Adamo, J. Jaramillo, R. Gomperts, R. E. Stratmann, O. Yazyev, A. J. Austin, R. Cammi,
591 C. Pomelli, J. W. Ochterski, P. Y. Ayala, K. Morokuma, G. A. Voth, P. Salvador,
592 J. J. Dannenberg, V. G. Zakrzewski, S. Dapprich, A. D. Daniels, M. C. Strain, O. Farkas,
593 D. K. Malick, A. D. Rabuck, K. Raghavachari, J. B. Foresman, J. V. Ortiz, Q. Cui, A. G.
594 Baboul, S. Clifford, J. Cioslowski, B. B. Stefanov, G. Liu, A. Liashenko, P. Piskorz,
595 I. Komaromi, R. L. Martin, D. J. Fox, T. Keith, M. A. Al-Laham, C. Y. Peng, A. Nanayakkara,
596 M. Challacombe, P. M. V. Gill, B. Johnson, W. Chen, M. W. Wong, C. Gonzalez and
597 J. A. Pople, Gaussian 03, Revision A.1, Gaussian, Inc., Pittsburgh, PA, 2003.
598 [12] G. Schaftenaar and J. H. Noordik, Molden: a pre- and post-processing program for molecular
599 and electronic structures. *J. Comput.-Aided Mol. Des.*, 2000, **14**, 123.
600 [13] S. Nourbakhsh, K. Norwood, H.-M. Yin, C.-L. Liao and C. Y. Ng, *J. Chem. Phys.*, 1991, **95**,
601 5014.
602 [14] J. Simons, P. Skurski and R. Barrios, *J. Am. Chem. Soc.*, 2000, **122**, 11893.
603 [15] This estimate is obtained by equating the intrinsic instability of the anion (3.80 eV) to the
604 Coulomb model's prediction of stabilization $2(14.4/(R+1.82/2))$ in eV.
605
606
607
608
609
610
611